

# Crystallization behaviour of calcium aluminate glass fibres

## Part I Differential thermal analysis study

YUN-MO SUNG\*

Department of Materials Science and Engineering, Daejin University, Pocheon-koon, Kyönggi-do 487-711, South Korea  
E-mail: ymsung@road.deejin.ac.kr

JIN-HEE SUNG

Paekche College, Wanjuo-koon, Chonbook 565-900, South Korea

Crystallization behaviour of as-spun and fully-nucleated calcium aluminate (CA) glass fibres produced via inviscid melt spinning (IMS), was studied. Differential thermal analysis (DTA) scans on the as-spun and fully-nucleated CA fibres were performed at different heating rates. By applying the Kissinger method to the DTA scan data the activation energy values for crystallization were determined to be 569 and 546 kJ mol<sup>-1</sup>, respectively for the as-spun and fully-nucleated CA fibres. The Ozawa analysis on the DTA scan data gave the Avrami parameters at 2.7 and 2.4, respectively, for the as-spun and fully-nucleated CA fibres, which indicates high tendency of bulk crystallization mode. The formation of equilibrium phases of Ca<sub>12</sub>Al<sub>14</sub>O<sub>33</sub> and CaAl<sub>2</sub>O<sub>4</sub> in the crystallized CA fibres was identified by using X-ray diffraction (XRD). © 1998 Kluwer Academic Publishers

### 1. Introduction

For many years calcium aluminate (CA) glasses have been recognized as candidates for optical materials and composite reinforcements [1–9]. They show sapphire-like infrared transmission, i.e. cutoff of about 6 μm, whereas silicate glasses present strong absorption in the 3 to 5 μm region [1–3]. The CA glasses are low-loss optical materials, showing scattering value of approximately 0.04 dB km<sup>-1</sup> at 1.55 μm [4]. It is considerably low compared to that of silicate glasses, 0.16 dB km<sup>-1</sup>. The CA glasses are also applicable to photometric devices since they are photosensitive to ultraviolet radiation [5].

On the other hand, the CA glasses in fibre form are promising reinforcements of cement [6], aluminium alloys [7, 8], and glass-ceramics [9]. The elastic modulus values of the CA fibres are higher than those of S- and E-glass fibres. In addition, they show prominent chemical stability and appropriate bonding with those matrices. Accordingly, the composites reinforced with the CA fibres reveal much improved mechanical responses compared to the matrix materials.

Crystallization is a critical limitation not only in the production, but in the application of the CA glasses in various forms due to their easiness of crystallization [10–13]. Once crystallization initiates their optical and mechanical properties would be seriously deteriorated. The glass formation and crystallization behaviour of the CaO–Al<sub>2</sub>O<sub>3</sub> composition has been studied. McMillan

and Piriou [10] found that the calcium aluminate can form glass at the composition range from 35.5 to 56.2 wt % CaO with rapid melt quenching. Uhlmann *et al.* [11] prepared calcium aluminate glasses based on the composition of 49.4 wt % CaO–50.6 wt % Al<sub>2</sub>O<sub>3</sub>. Their results showed that by air cooling only the small size (~7 g) calcium aluminate melt forms clear glass, and the bigger size melt (≥20 g) forms at least partially crystalline glass or full crystal. Wallenberger *et al.* [12] studied crystallization of calcium aluminate (CA) fibres of 39.0 wt % CaO–61.0 wt % Al<sub>2</sub>O<sub>3</sub> with heat treatment of 1200 °C for 1 h. Their results indicate almost complete crystallization of Ca<sub>12</sub>Al<sub>14</sub>O<sub>33</sub> and CaAl<sub>2</sub>O<sub>4</sub> as major phases. Mitchell *et al.* [13] heat treated vitreous CA fibres of eutectic composition (46.5 wt % CaO–53.5 wt % Al<sub>2</sub>O<sub>3</sub>) at 900, 1000 and 1100 °C for 6–6000 s to characterize the crystallization process. The results show the presence of Ca<sub>12</sub>Al<sub>14</sub>O<sub>33</sub>, Ca<sub>3</sub>Al<sub>10</sub>O<sub>18</sub>, and CaAl<sub>4</sub>O<sub>7</sub> with different amounts in all crystallized fibres.

The CA fibres of low eutectic composition (46.5 wt % CaO–53.5 wt % Al<sub>2</sub>O<sub>3</sub>) were fabricated using inviscid melt spinning (IMS) [14–16] which is the unique method of producing ceramic fibres directly from low-viscosity melts (<10 Pa s). This study was performed to investigate the detail crystallization behaviour of as-spun and fully nucleated CA glass fibres by using differential thermal analysis (DTA). The DTA results were carefully analysed to estimate the activation energy for

\* Author to whom all correspondence should be addressed.

crystallization and crystallization mode of the CA fibres. X-ray diffraction (XRD) was also employed to identify crystallinity of the fully nucleated and crystallized CA fibres.

## 2. Experimental procedure

The detail procedure of the CA fibre fabrication via inviscid melt spinning (IMS) has been described previously [14–16]. For DTA (Setaram TGDTA-92, France) experiments the as-spun CA fibres were carefully cut to 7 mm in length using a razor blade. A portion (20 mg) of the chopped CA fibres was loaded inside a platinum cup for each DTA scan and alumina powder was used as a reference. The DTA scans were performed in an air atmosphere and at the heating rates of 10, 15, 20, 30, 40 and 60 °C min<sup>-1</sup>. The scan temperatures ranged from 600 to 1200 °C. The DTA temperatures were calibrated using pure aluminium and copper. Kissinger and Ozawa analyses were applied to the DTA scan results to obtain the activation energy for crystallization and the crystallization mode of the as-spun CA fibres, respectively.

The as-spun CA fibres were heat treated isothermally at the glass transition temperature ( $T_g$ ) for 1, 2, 4 and 6 h, respectively, for complete nucleation. The CA fibres heat treated for each time period were analysed by DTA to find the time for complete nucleation. The time needed for complete nucleation of the as-spun CA fibres was determined by examining the saturation in the crystallization peak temperatures according to the time period of nucleation heat treatment.

The as-spun CA fibres were heat treated for the time period required for complete nucleation to prevent the increase in the number of nuclei during the DTA scans. DTA scans on the fully nucleated CA fibres were performed at the heating rates of 10, 15, 20, 30, 40 and 60 °C min<sup>-1</sup>. The activation energy for crystallization and the crystallization mode of the fully nucleated CA fibres were identified by analysing the DTA scan data. In order to identify the crystallinity in the fully nucleated and crystallized CA fibres the powdered CA fibres were investigated using XRD (Nicolet Stoe Transmission/Bragg-Brentano, Germany) with a CuK $\alpha$  source, a 5-s time constant, a 10–70° scan, and 0.05° step size.

## 3. Results and discussion

### 3.1. Crystallization behaviour of as-spun CA fibres

In order to investigate crystallization behaviour of the as-spun CA fibres, DTA scans were performed at the heating rates of 10, 15, 20, 30, 40 and 60 °C min<sup>-1</sup>. Fig. 1 shows the DTA scan curves. The faster the heating rates, the higher the peak temperatures and the larger the peak heights become. The variation of the crystallization peaks according to the DTA scan rates can be used to estimate the activation energy for crystallization and crystallization mode. The activation energy

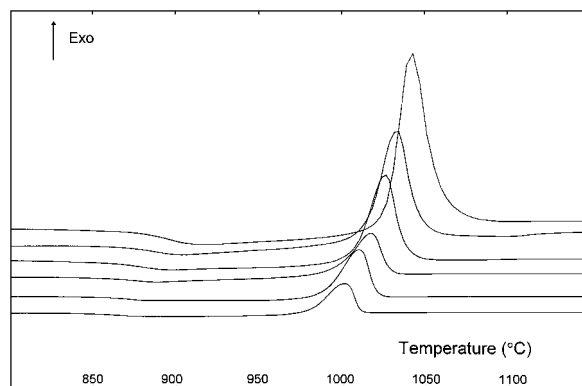


Figure 1 Differential thermal analysis (DTA) scan curves of as-spun CaO–Al<sub>2</sub>O<sub>3</sub> (CA) fibres. Each of the scan curves from the bottom to the top corresponds to the respective heating rate of 10, 15, 20, 30, 40 and 60 °C min<sup>-1</sup>.

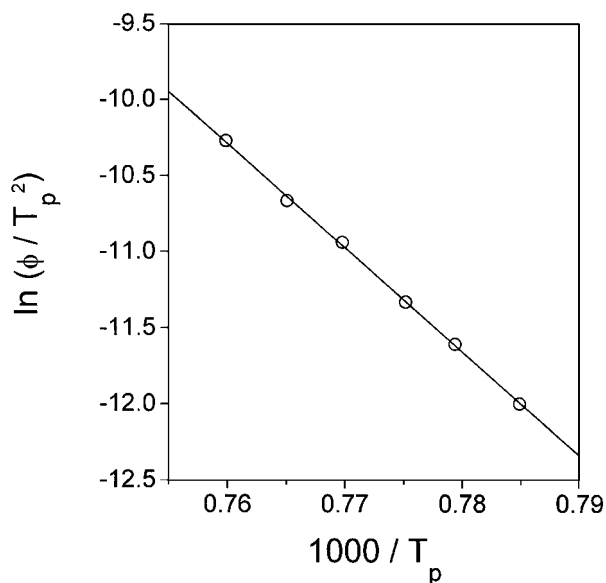


Figure 2 Kissinger plot of as-spun CaO–Al<sub>2</sub>O<sub>3</sub> (CA) fibres with DTA heating rates of 10, 15, 20, 30, 40 and 60 °C min<sup>-1</sup>. From the slope of the curve the activation energy for crystallization of the fibres was determined to be 569 kJ mol<sup>-1</sup>.

for the crystallization of the CA fibres can be estimated by using following Kissinger analysis [17]

$$\ln\left(\frac{\phi}{T_p^2}\right) = -\frac{E_{ck}}{RT_p} + \text{const.} \quad (1)$$

where  $\phi$  is the DTA scan rate;  $T_p$  is the crystallization peak temperature;  $E_{ck}$  is the activation energy for crystallization estimated by Kissinger method; and  $R$  is the gas constant. By substituting  $\phi$  values and corresponding  $T_p$  values into the Equation 1 the Kissinger plot of the as-spun CA fibres was obtained and presented in Fig. 2. From the slope of the Kissinger plot the activation energy for the crystallization of the as-spun CA fibres was determined as 569 kJ mol<sup>-1</sup>.

The crystallization mode of a glass has a practical importance in the usage of it and also in the fabrication of a glass-ceramic since the surface crystallization mode may introduce huge thermal expansion difference at the boundary between the glass phase and

crystallized phase, building up high tensile stress. This high tensile stress at the interface mostly causes total failure of the glass. On the other hand, in the case of the bulk crystallization mode where the crystal growth occurs at the finely distributed precursor nuclei in the glass, the huge thermal expansion coefficient gradient across the whole glass body does not occur, and the glass body is safe against the thermal failure. Thus, from this perspective the bulk crystallization is desirable compared to the surface crystallization. It is well known that in the production of glass-ceramics, nucleation agents such as  $\text{TiO}_2$  and/or  $\text{ZrO}_2$  are used to form titanates or zirconates finely distributed in a glass body [18, 19]. These precursor-nuclei finely distributed in a glass body cause bulk crystallization and thus a sound glass-ceramic body can be produced without a failure. The crystallization mode can be identified by using following Ozawa analysis [20]

$$\{\ln[-\ln(1-x)]\}_T = -n \ln \phi + \text{const.} \quad (2)$$

where  $x$  is the volume fraction crystallized at a fixed temperature  $T$  ( $1020^\circ\text{C}$ ) when heated at  $\phi$  that is, the ratio of the partial area at  $T$  to the total area of the crystallization exotherm;  $n$  is the Avrami parameter which indicating crystallization mode. When surface crystallization dominates,  $n = 1$ , and when bulk crystallization dominates,  $n = 3$ . When both the surface and bulk crystallization occur  $n$  has a value between 1 and 3. By substituting  $\phi$  values and corresponding  $x$  values into Equation 2 the Ozawa plot of the as-spun CA fibres was created in Fig. 3. From the slope of the Ozawa plot the Avrami parameter of the as-spun CA fibres was determined as 2.7 which implies apparent bulk crystallization mode with small portion of surface crystallization.

The existence of precursor nuclei inside the as-spun CA fibres is certain as they show high tendency of bulk

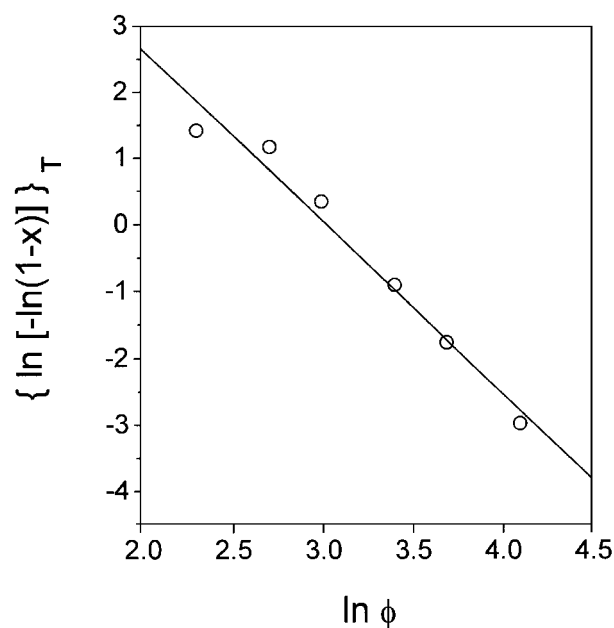


Figure 3 Ozawa plot of as-spun  $\text{CaO-Al}_2\text{O}_3$  (CA) fibres. The “ $x$ ” indicates the volume fraction crystallized to  $1020^\circ\text{C}$ . From the slope of the curve the Avrami parameter ( $n$ ) of the fibres was determined as 2.7.

crystallization mode. The nature of the precursor nuclei inside the fibres is not clear at this time. It is likely that they are prematurely formed calcium aluminates such as  $\text{Ca}_{12}\text{Al}_{14}\text{O}_{33}$  and  $\text{CaAl}_2\text{O}_4$  because the CA glass fibres were produced via inviscid melt spinning (IMS) by which the glass melt was air cooled, and the cooling rate would have not been so fast to avoid the formation of precursor nuclei. It is also likely that the nuclei would be the compound possibly formed by the reaction between the starting powders ( $\text{CaO}$  and/or  $\text{Al}_2\text{O}_3$ ) and an impurity oxide possibly included in them. Transmission electron microscopy (TEM) work will be performed to identify the nature of the precursor nuclei and will be reported in Part II.

### 3.2. Crystallization behaviour of fully-crystallized CA fibres

Matusita and Sakka [21] mentioned that the Kissinger equation is valid only when the number of nuclei is fixed during crystal growth. If most of the nuclei are formed during the DTA scan, the activation energy values from the Kissinger equation are incorrect. Thus, for present study the as-spun CA fibres were completely nucleated at the glass transition temperature and the crystallization behaviour of these nucleated CA fibres were examined by using DTA scans. The glass transition temperature ( $T_g$ ) of  $869^\circ\text{C}$  and crystallization peak temperature ( $T_p$ ) of  $1017^\circ\text{C}$  at the heating rate of  $20^\circ\text{C min}^{-1}$  were used as references. By using DTA the as-spun CA fibres were rate-heated ( $20^\circ\text{C min}^{-1}$ ) to  $869^\circ\text{C}$  and hold for 1, 2, 4 and 6 h, respectively, for nucleation. The DTA scans on the CA fibres nucleated at each time period were performed at a heating rate of  $20^\circ\text{C min}^{-1}$ , and the  $T_p$  values of each CA fibre were plotted as a function of nucleation time in Fig. 4. There is no further decrease in the  $T_p$  values of the CA fibres nucleated for longer than 4 h. It would be

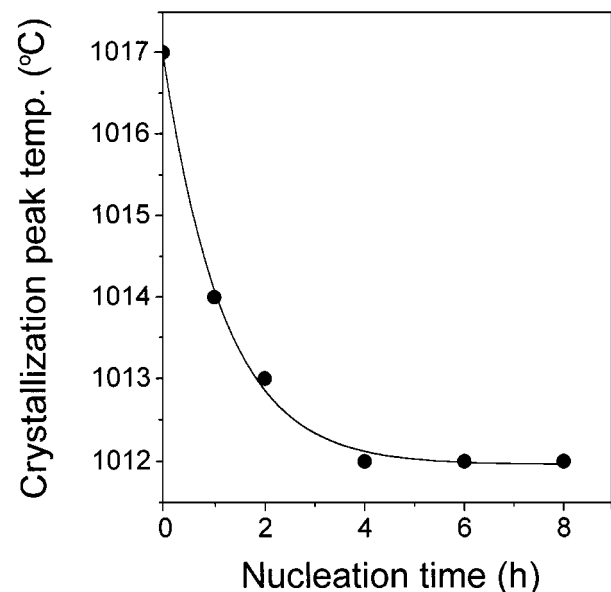


Figure 4 Crystallization peak temperatures ( $T_p$ ) of the nucleated CA fibres according to the nucleation heat treatment time. They show the saturation at around 4 h nucleation.

TABLE I Variation of the crystallization peak temperatures ( $T_p$ ) of the as-spun and fully nucleated CaO–Al<sub>2</sub>O<sub>3</sub> (CA) fibres according to the DTA scan rates

CA fibres	$T_p$ (°C)					
	DTA scan rates (°C min <sup>-1</sup> )					
	10	15	20	30	40	60
As-spun CA	1001	1010	1017	1026	1034	1043
Fully nucleated CA	997	1006	1012	1022	1029	1041

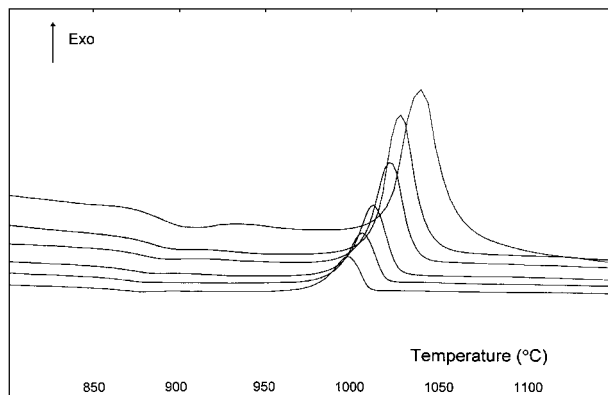


Figure 5 Differential thermal analysis (DTA) scan curves of completely nucleated CaO–Al<sub>2</sub>O<sub>3</sub> (CA) fibres. Each of the scan curves from the bottom to the top corresponds to the respective heating rate of 10, 15, 20, 30, 40 and 60 °C min<sup>-1</sup>.

concluded that the nucleation is completed at around 4 h heat treatment. Thus, the as-spun CA fibres were heat treated for complete nucleation at 869 °C for 5 h.

DTA scans on the CA fibres completely nucleated were performed at heating rates of 10, 15, 20, 30, 40 60 °C min<sup>-1</sup>, and the corresponding DTA scan curves are shown in Fig. 5. Table I lists the crystallization peak temperatures ( $T_p$ s) of both the as-spun and fully-nucleated CA fibres according to the DTA scan rates. There is about 4 °C difference in each of the  $T_p$  values of the two fibres. The decreased  $T_p$  values in the nucleated CA fibres would result from the increased number of nuclei.

In order to get the activation energy for crystallization of the CA fibres completely nucleated the Kissinger method (Equation 1) was applied. Fig. 6 shows the Kissinger plot of the fully-nucleated CA fibres, and from the slope of the curve the activation energy for crystallization,  $E_{ck}$  was determined as 546 kJ mol<sup>-1</sup> for the CA fibres completely nucleated at 869 °C. This activation energy is slightly lower than that of the as-spun CA fibres and would result from the increased number of nuclei.

Fig. 7 shows the Ozawa plot of the fully nucleated CA fibres. From the slope of the plot the Avrami parameter for the fully nucleated CA fibres was determined as 2.4. This implies that the nucleated CA fibres crystallize mostly by the bulk crystallization mode. The slightly decreased  $n$  value of the fully nucleated CA fibres compared to that of the as-spun CA fibres indicates the enhanced tendency of surface crystallization, and this would come from the increased number of precursor nuclei at the surface of the CA glass fibre. This

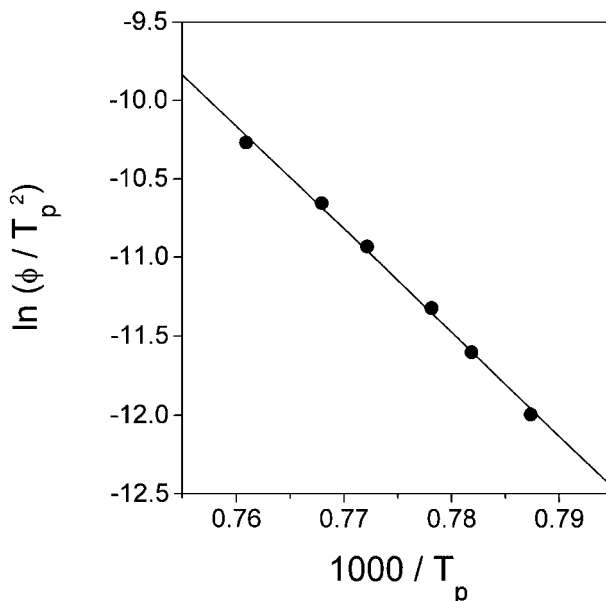


Figure 6 Kissinger plot of completely nucleated CaO–Al<sub>2</sub>O<sub>3</sub> (CA) fibres with DTA heating rates of 10, 15, 20, 30, 40 and 60 °C min<sup>-1</sup>. From the slope of the curve the activation energy for crystallization of the fibres was determined to be 546 kJ mol<sup>-1</sup>.

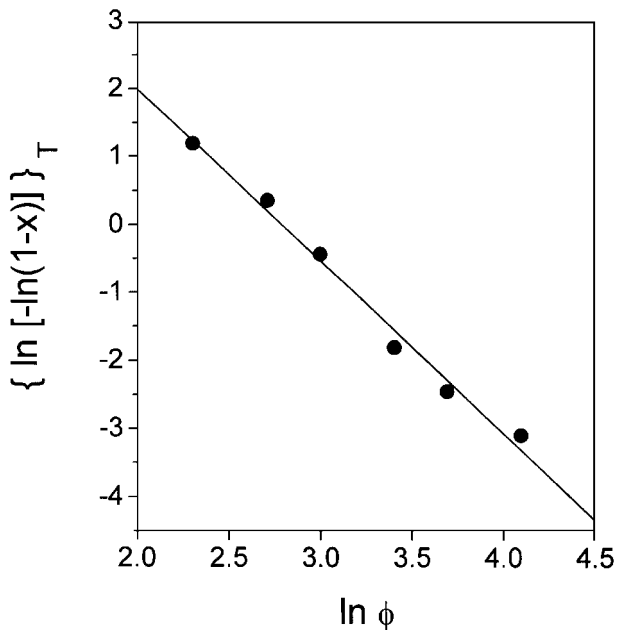


Figure 7 Ozawa plot of as-spun CaO–Al<sub>2</sub>O<sub>3</sub> (CA) fibres. The “x” indicates the volume fraction crystallized to 1010 °C. From the slope of the curve the Avrami parameter ( $n$ ) of the fibres was determined as 2.4.

situation implies that there were fixed number of precursor nuclei in the glass body, and their number did not change by the nucleation heat treatment while at the surface new nuclei were formed by the nucleation heat treatment. This scenario will be confirmed using TEM analysis and will be reported in the Part II of this study.

### 3.3. X-ray diffraction (XRD) analyses of the CA fibres

XRD was performed to examine the crystallinity and to identify the crystalline phases of both the fully nucleated and crystallized CA fibres. The XRD patterns

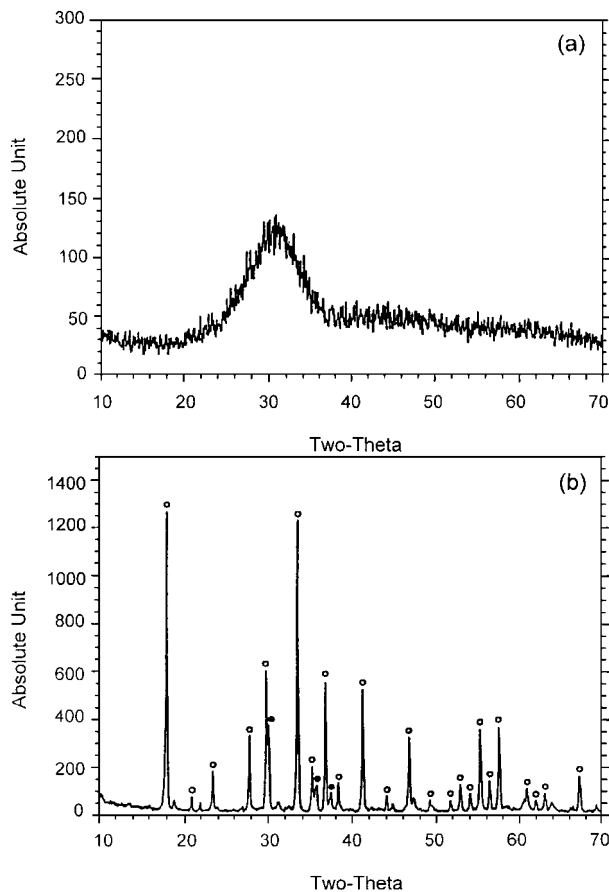


Figure 8 X-ray diffraction (XRD) patterns of the CaO–Al<sub>2</sub>O<sub>3</sub> (CA) fibres: (a) fully nucleated at 869 °C for 5 h and (b) crystallized during the DTA scan (10 °C min<sup>-1</sup>) up to 1200 °C. By comparing the peak positions and intensities with the data in JCPDS cards the crystalline phases of Ca<sub>12</sub>Al<sub>14</sub>O<sub>33</sub>(○) and CaAl<sub>2</sub>O<sub>4</sub>(●) were identified in the CA fibres.

of the CA fibres (a) fully nucleated 869 °C for 5 h and (b) crystallized during the DTA scan (10 °C min<sup>-1</sup>) up to 1200 °C, are shown in Fig. 8. For the XRD pattern of the fully nucleated CA fibres there is a broad hill ranging from approximately 20 to 40°, indicating clear non-crystallinity. Any distinct peak representing crystallinity was not detected in the XRD pattern, which implies that the CA fibres were not crystallized during the nucleation heat treatment.

For the XRD pattern of the crystallized CA fibres many peaks presenting the formation of crystalline phases were found. The two major crystalline phases of Ca<sub>12</sub>Al<sub>14</sub>O<sub>33</sub> and CaAl<sub>2</sub>O<sub>4</sub> which were expected from the equilibrium phase diagram of the CaO–Al<sub>2</sub>O<sub>3</sub> system, were identified by comparing the peak positions and intensities of the XRD pattern with the data in the JCPDS cards. The broad hill presenting the existence of amorphous phase had disappeared, which indicates almost complete crystallization of the CA fibres.

#### 4. Conclusions

The detail crystallization behaviour of the as-spun and fully-nucleated CaO–Al<sub>2</sub>O<sub>3</sub> glass fibres was studied using DTA and XRD. The Kissinger analyses on both the

CA fibres showed the slightly decreased activation energy value for crystallization for the fully nucleated CA fibres (546 kJ mol<sup>-1</sup>) compared to the as-spun CA fibres (569 kJ mol<sup>-1</sup>). The Ozawa analyses on both the CA fibres revealed that both the CA fibres would crystallize mostly by bulk crystallization mode together with a small portion of surface crystallization. The fully nucleated CA fibres were expected to show slightly higher tendency of surface crystallization (Avrami parameter of 2.4) compared to the as-spun CA fibres (Avrami parameter of 2.7) most probably caused by the increased number of precursor nuclei at the surface of glass fibres. The equilibrium crystalline phases of Ca<sub>12</sub>Al<sub>14</sub>O<sub>33</sub> and CaAl<sub>2</sub>O<sub>4</sub> were identified in the crystallized CA fibres by using XRD.

#### Acknowledgements

The author would like to thank Ms Hye-Juan Park at Daejin University, Kyunggi-do, Korea for helping performing experiments. This study was partially supported by Daejin University Research Grants in 1998.

#### References

1. H. C. HAFNER, N. J. KREIDL and R. A. WEIDEL, *J. Amer. Ceram. Soc.* **41** (1958) 315.
2. J. R. DAVY, *Glass Technol.* **19** (1978) 32.
3. F. T. WALLENBERGER, N. E. WESTON and S. A. DUNN, *J. Non-Cryst. Solids* **124** (1990) 116.
4. M. E. LINES, J. B. MACCHESNEY, K. B. LYONS, A. J. BRUCE, A. E. MILLER and K. NASSAU, *ibid.* **107** (1989) 251.
5. H. HOSONO, K. YAMAZAKI and Y. ABE, *J. Amer. Ceram. Soc.* **68** (1985) C-304.
6. K.-Y. YON, B. S. MITCHELL, S. A. DUNN and J. A. KOUTSKY, *Cement & Concrete Composites* **15** (1993) 165.
7. Y.-M. SUNG, K.-Y. YON, S. A. DUNN and J. A. KOUTSKY, *J. Mater. Sci.* **29** (1994) 5583.
8. Y.-M. SUNG, *ibid.* **32** (1997) 1069.
9. Y.-M. SUNG and J.-H. SUNG, *J. Mater. Sci. Lett.* **16** (1997) 1527.
10. P. MCMILLANN and B. PIRIOU, *J. Non-Cryst. Solids* **55** (1983) 221.
11. E. V. UHLMANN, M. C. WEINBERG, N. J. KREIDL and A. A. GOKTAS, *J. Amer. Ceram. Soc.* **76** (1993) 449.
12. F. T. WALLENBERGER, N. E. WESTON and S. A. DUNN, *SAMPE Quart.* **21** (1990) 30.
13. B. S. MITCHELL, K.-Y. YON, S. A. DUNN and J. A. KOUTSKY, *J. Non-Cryst. Solids* **152** (1993) 143.
14. Y.-M. SUNG, S. A. DUNN and J. A. KOUTSKY, *J. Mater. Sci.* **30** (1995) 5995.
15. Y.-M. SUNG and S. A. DUNN, *ibid.* **31** (1996) 3657.
16. *Idem.*, *ibid.* **31** (1996) 4741.
17. H. E. KISSINGER, *J. Res. Natl. Bur. Stand.* **57** (1956) 217.
18. Y.-M. SUNG, S. A. DUNN and J. A. KOUTSKY, *J. Eur. Ceram. Soc.* **14** (1994) 455.
19. Y.-M. SUNG, *J. Mater. Sci.* **31** (1996) 5421.
20. T. OZAWA, *Polymer* **12** (1971) 150.
21. K. MATUSITA and S. SAKKA, *J. Non-Cryst. Solids* **38–39** (1980) 741.

Received 10 March  
and accepted 17 July 1998